BrainSegDMlF: A Dynamic Fusion-enhanced SAM for Brain Lesion Segmentation

Hongming Wang*
Yifeng Wu*
12333530@mail.sustech.edu.cn
3049421927@qq.com
Southern University of Science and Technology
Nanshan Qu, Shenzhen, China

Huimin Huang
Tencent
Shenzhen, China

Hongtao Wu
Westlake University
Hangzhou, China

Jia-Xuan Jiang
Westlake University
Hangzhou, China

Xiaodong Zhang
Shenzhen Institutes of Advanced Technology, Chinese Academy of Sciences, Chinese Academy of Sciences
Shenzhen, China

Hao Zheng
Youtu Lab, Tencent
Shenzhen, China

Xian Wu
Tencent
Shenzhen, China

Yefeng Zheng
Westlake University
Hangzhou, China

Yefeng Zheng
Westlake University
Hangzhou, China

Jinping Xu
Shenzhen Institutes of Advanced Technology, Chinese Academy of Sciences, Chinese Academy of Sciences
Shenzhen, China

Jing Cheng
Shenzhen Institutes of Advanced Technology, Chinese Academy of Sciences, Chinese Academy of Sciences
Shenzhen, China

arXiv:2505.06133v1 [cs.CV] 9 May 2025

Abstract

The segmentation of substantial brain lesions is a significant and challenging task in the field of medical image segmentation. Substantial brain lesions in brain imaging exhibit high heterogeneity, with indistinct boundaries between lesion regions and normal brain tissue. Small lesions in single slices are difficult to identify, making the accurate and reproducible segmentation of abnormal regions, as well as their feature description, highly complex. Existing methods have the following limitations: 1) They rely solely on single-modal information for learning, neglecting the multi-modal information commonly used in diagnosis. This hampers the ability to comprehensively acquire brain lesion information from multiple perspectives and prevents the effective integration and utilization of multi-modal data inputs, thereby limiting a holistic understanding of lesions. 2) They are constrained by the amount of data available, leading to low sensitivity to small lesions and difficulty in detecting subtle pathological changes. 3) Current SAM-based models rely on external prompts, which cannot achieve automatic segmentation and, to some extent, affect diagnostic efficiency.To address these issues, we have developed a large-scale fully automated segmentation model specifically designed for brain lesion segmentation, named BrainSegDMLF. This model has the following features: 1) Dynamic Modal Interactive Fusion (DMIF) module that processes and integrates multi-modal data during the encoding process, providing the SAM encoder with more comprehensive modal information. 2) Layer-by-Layer Upsampling Decoder, enabling the model to extract rich low-level and high-level features even with limited data, thereby detecting the presence of small lesions. 3) Automatic segmentation masks, allowing the model to generate lesion masks automatically without requiring manual prompts.We tested and evaluated our model on two common brain disease segmentation benchmarks, including cases of focal cortical dysplasia and gliomas. Our model outperformed existing state-of-the-art methods across four metrics.

CCS Concepts

• **Computing methodologies → Image segmentation**;

*Both authors contributed equally to this research.

Permission to make digital or hard copies of all or part of this work for personal or classroom use is granted without fee provided that copies are not made or distributed for profit or commercial advantage and that copies bear this notice and the full citation on the first page. Copyrights for components of this work owned by others than the author(s) must be honored. Abstracting with credit is permitted. To copy otherwise, or republish, to post on servers or to redistribute to lists, requires prior specific permission and/or a fee. Request permissions from permissions@acm.org.
MM '25, Dublin, Ireland
© 2025 Copyright held by the owner/author(s). Publication rights licensed to ACM.
ACM ISBN 978-1-4503-XXXX-X/2018/06
https://doi.org/XXXXXXX.XXXXXXX

Keywords

Multi-modality image segmentation, Cross-modality interaction, Medical Image Segmentation

1 Introduction

Brain parenchymal lesions represent one of the most severe and complex challenges in the medical field, encompassing tumors, vascular diseases, trauma, and other conditions that may be congenital or acquired. These diseases significantly impact people's health and safety. Segmentation constitutes the initial stage in the treatment planning of brain parenchymal lesions [16, 22] , playing a crucial role in the diagnosis, treatment, and monitoring of various diseases. This stage primarily relies on physicians manually delineating lesion regions [16] , which requires substantial time and professional expertise. Due to the heterogeneity of lesions, blurred boundaries, and diverse morphological characteristics, segmentation becomes challenging, resulting in inconsistencies in the size of regions manually segmented by different physicians [13, 14] . Computer-assisted brain parenchymal lesion segmentation represents a particularly important method that can help hospitals and patients save considerable time in disease detection, improve physician efficiency and treatment success rates, and eliminate issues of segmentation inconsistency.

In recent years, deep learning, as a significant artificial intelligence method, has been increasingly applied to medical image segmentation [10, 11, 26], becoming a powerful approach in medical image processing. Deep learning models such as U-net and its variants have demonstrated excellent performance and accuracy in medical image segmentation [9, 11, 26] . Although these convolutional neural network-based methods are effective in extracting local image features, they are limited by their local receptive fields [19],making them unable to utilize global contextual information and process long-range dependencies in image data. Recent studies have proposed Vision Transformers (ViTs), which have made significant progress in addressing global context and long-range dependency problems [8, 23]. Based on improvements to ViTs, several highly effective models have emerged, such as SwinUNet [3]. Notably, in the field of medical image segmentation, models like UNETR and nnFormer[7, 36] have demonstrated outstanding performance.However, both CNN-based and ViT-based models require large amounts of annotated data, which presents a major challenge in the medical field. Considering the similarities between segmentation tasks, using pre-trained weights from natural image models has become possible.

The Segment Anything Model (SAM) [15], developed by Meta AI, consists of a Transformer-based image encoder coupled with a lightweight decoder. As a novel foundational visual segmentation model trained on billions of images, it has shown tremendous potential in medical imaging, particularly in segmenting organs with clear boundaries [4]. However, due to the heterogeneity and blurred boundaries characteristic of lesions, significant challenges exist in lesion segmentation, especially for small lesions. Given SAM's relatively simple decoder structure and the small proportion of minor lesions in images, whose shape, texture, and other features are less distinct compared to normal lesions, SAM may fail to clearly recognize or segment small lesions, particularly with medical image datasets that are typically limited in scale and diversity. SAM was designed considering only single-modality image input, without accounting for multi-modal data input possibilities, resulting in deficiencies in multi-modal data processing and limiting its learning to single-modality data with only simple processing for multi-modal data.

In the examination of brain parenchymal lesions, Magnetic Resonance Imaging (MRI) has become the core basis for clinical diagnosis and treatment decisions. As a high-resolution imaging technology, MRI offers multi-modal imaging capabilities, clearly displaying subtle changes in brain structures. Clinicians typically analyze multiple MRI sequence parameters comprehensively to achieve a thorough assessment of the patient's condition. Common MRI modalities include T1, T2, FLAIR, as shown in Figure 1. Single-modality MRI has inherent limitations in displaying lesion boundaries and features, making it difficult to fully characterize heterogeneous lesion features [18]. Although multi-modal data contains rich complementary information, many current research methods have not fully exploited its potential, with most simply using multi-modal data as direct input to models [17], lacking effective multi-modal information fusion strategies. This simplified processing approach limits the model's ability to learn and integrate lesion information from multiple perspectives, resulting in underutilization of valuable data resources.

To address the above challenges in brain lesion segmentation, we propose BrainSegDMIF—a fully automatic 2D brain parenchymal lesion segmentation model that incorporates multi-modal and multi-scale capabilities based on SAM. This model inherits SAM's powerful architecture while innovatively designing a multi-modal fusion module in the Encoder section to effectively integrate and transmit information across different modalities. This module efficiently extracts and integrates multi-modal features, capturing complementary information of the same lesion from different perspectives. By fully utilizing the complementary advantages of multi-modal data, it enables SAM to simultaneously learn information from multiple modalities during encoding, understanding image content from different perspectives. To address the model's insufficient sensitivity in recognizing small lesions, we further designed a layer-by-layer upsampling decoder that employs a multi-scale feature fusion strategy, systematically restoring the spatial resolution of deep feature maps extracted during the model's encoding phase while preserving rich semantic information of the image data. We also optimized SAM's functionality to automatically generate lesion masks without prompts.

Our main contributions can be summarized as follows:

- In response to SAM's insufficient utilization of multi-modal data, we designed an efficient multi-modal image fusion module (DMIF) that integrates multi-modal image data during the image encoding stage, enhancing the model's image comprehension capabilities.
- Addressing the heterogeneity, blurred boundaries, and poor visualization of small lesions, we designed a layer-by-layer upsampling decoder that employs a multi-scale information fusion strategy to enhance the model's segmentation accuracy and sensitivity to lesions.

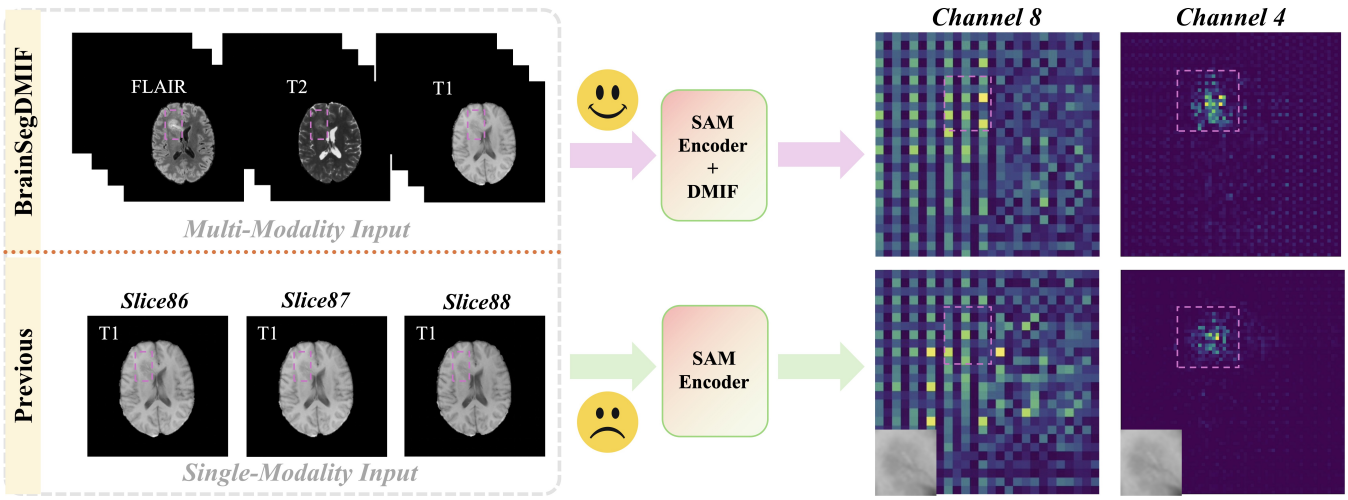

Figure 1: The figure compares feature extraction using multimodal versus unimodal data, showing that the encoder with a modality fusion module can better learn lesion features and clearly distinguish between lesion and non-lesion regions. The left panel shows multimodal brain lesion images, while the right panel displays lesion features extracted using different methods. Features extracted from unimodal data are more dispersed, making it difficult to distinguish between lesion and non-lesion regions. In contrast, after multimodal fusion using the DMIF module, lesion regions appear significantly brighter and features are more concentrated, indicating improved feature quality and enhanced lesion recognition.

- By optimizing SAM, our model can automatically generate high-quality image segmentation masks without prompts, eliminating the traditional SAM's dependence on clicking, boxing, or text prompts, thereby improving the model's practicality and efficiency in real-world application scenarios.

2 Related Work

2.1 SAM in Medical Image Analysis

Large foundation models represent one of the most dynamic and rapidly evolving domains in artificial intelligence research. These models aim to solve diverse human-world problems by developing extensive frameworks that utilize vast amounts of data to train large-scale vision or language models, enabling them to learn universal representations and functionalities. As a novel foundational visual segmentation model, SAM (Segment Anything Model) has demonstrated exceptional unsupervised and zero-shot generalization capabilities through training on the extensive SA-1B dataset.

Despite SAM's significant advances in natural image segmentation, it encounters substantial performance issues when applied to medical image segmentation tasks [2, 5, 20]. This performance gap primarily stems from the severe underrepresentation of medical domain data in the SA-1B dataset compared to the abundance of natural images [32]. This data imbalance has prevented SAM from learning sufficient anatomical structure representations in the medical domain, which are crucial for reliable medical image understanding.

Consequently, adapting SAM to the medical image segmentation domain has emerged as a significant research direction. Numerous efforts have been made to optimize SAM specifically for medical tasks [20, 30, 34]. Current researchers typically employ either comprehensive fine-tuning or parameter-efficient fine-tuning methods to adapt SAM to medical domain tasks. Comprehensive fine-tuning involves thorough parameter adjustments of the pre-trained model, typically updating most or all model parameters to better suit specific tasks or domains. Through comprehensive fine-tuning of vanilla SAM on large medical datasets, researchers have achieved state-of-the-art (SOTA) results [20]. However, comprehensive fine-tuning demands substantial memory resources and computational power, although research indicates that transferring pre-trained models to medical imaging tasks is highly feasible [24].

Parameter-efficient fine-tuning methods achieve efficient model adaptation by updating only a small portion of parameters in pre-trained models. Unlike comprehensive fine-tuning, this approach freezes the majority of parameters and only learns an extremely small subset, typically less than 5% of the total parameter count. Current research predominantly focuses on fine-tuning SAM with specific medical segmentation datasets to adapt it to particular tasks. Wu et al. [30]proposed MSA, a straightforward adapter technique that integrates specific medical domain knowledge into SAM by inserting adapters into the original model, thereby enhancing its capabilities in medical tasks. Zhang et al. [33] fine-tuned SAM's encoder component using LoRA while simultaneously fine-tuning the decoder for abdominal segmentation. Integrating SAM into medical image segmentation further involves model modifications and new module designs. Y Wu et al. [31] enabled SAM to adapt to lesion image segmentation by introducing LoRA and designing new decoder modules, thus addressing SAM's deficiencies in medical lesion recognition.

2.2 Multimodal medical image segmentation

Multimodal learning enhances model representation capability by leveraging multi-source information. Single-modality data is inherently limited and cannot comprehensively reflect physiological conditions. In clinical practice, multimodal imaging is widely used to support diagnosis. MRI, as the preferred modality for brain-related diseases, captures tissue characteristics and pathological information through sequences such as T1, T2, FLAIR, and T1CE, providing complementary perspectives.However, current research often focuses on improving image quality by incorporating auxiliary modalities as prior information into the target modality. For instance, Wang et al.[29] designed a cascaded architecture that combines multimodal data as input for brain tumor segmentation. Myronenko et al.[21] also integrated multimodal data as input, augmenting a U-Net architecture with a VAE branch for image reconstruction. Z. Jiang et al.[12] proposed a two-stage cascaded U-Net for segmenting multimodal brain tumor data. Y. Zhang[35] embedded multimodal CT images through a fully connected layer as input. Despite their effectiveness, these approaches fail to explore how to integrate complementary information from different modalities to form a unified and efficient representation.This has motivated us to investigate multimodal fusion in the context of image segmentation.

3 Methods

In the context of multi-modal medical image segmentation, we define the training set as $D_M = \{(x_i^M, y_i^M)\}_{i=1}^{n_M}$, where $x_i^M \in \mathbb{R}^{H\times W\times C}$ represents the i-th multi-modal sample, typically comprising image data from various modalities (such as MRI, CT, etc.), and $y_i^M \in \mathbb{R}^{H\times W}$ denotes its corresponding ground truth annotation. The term n_M indicates the number of training samples. The objective of this task is to maximize the similarity between the predicted labels $\overline{y}_i^T$ and an unseen multi-modal dataset $D_T = \{(x_i^T, y_i^T)\}_{i=1}^{n_T}$.

The proposed BrainSegDMIF architecture is illustrated in Figure 2, comprising three principal components: a modality fusion encoder, an automatic mask generator, and a progressive upsampling decoder. For each patient's multi-modal data x_i^M, we initially extract features through modality-specific encoders, yielding feature representations f_{s_1} , f_{s_2} , . . . , f_{s_m} across different modalities, where m denotes the number of modalities. These modal features are subsequently directed to the Dynamic Modality Interaction Fusion (DMIF) module, which adaptively generates fusion weights by integrating multi-modal data, performing weighted fusion of features from different modalities to enhance complementary information while suppressing redundant information. The fused features f_{fus} are transmitted during the encoding phase to each modality's encoder where they are integrated with the data learned by that specific encoder, compensating for learning limitations caused by information deficiencies in individual modalities, thereby enhancing the model's comprehension capability and representational efficacy for multi-modal data. The f_{fus} obtained from the final layer is further propagated to the decoder, where the multi-scale fusion mechanism of the decoder gradually increases the scale of the generated lesion mask, guiding model learning through loss function optimization and consequently improving segmentation accuracy.

3.1 Dynamic Modal Interactive Fusion

In clinical practice, multimodal imaging is widely used for disease diagnosis, and effectively utilizing multimodal data remains a fundamental challenge in medical image segmentation. To address this, we designed the Dynamic Modal Interactive Fusion (DMIF) module to aggregate medical imaging information from diverse modalities and provide lesion features from multiple perspectives to enhance model performance. The architecture of this module is illustrated in Figure 3.

The DMIF module consists of three key components: the inter-modal interaction module, the dynamic weight generation module, and the adaptive feature aggregation module. These components interact and fuse data to learn complementary information from multimodal data adaptively, enabling the model to accommodate multi-modal inputs.

Since most clinical multimodal data are image-based, we used a unified SAM Encoder for feature extraction and encoding to avoid inconsistencies in sequence length and feature dimensions caused by different extraction methods. Specifically, for an image x_i^m from modality m , we encoded it using multi-layer Vision Transformers (ViTs) to obtain features f_{s_1} , f_{s_2} , . . . , f_{s_m} at different layers. These features were combined into a high-dimensional feature tensor $f_i \in \mathbb{R}^{N\times D\times M}$ where i denotes the i-th layer. This process maps multi-modal data from their original domains into a unified feature space, forming a high-dimensional feature f_i that serves as input to the inter-modal interaction module. By unifying features into a shared space, we established a foundation for subsequent semantic alignment and feature interaction.

3.1.1 Intermodal interaction layer. The inter-modal interaction layer is designed to enable effective interaction and influence among features from different modalities. Multimodal data often originates from distinct data domains, each with unique characteristics and representations. For instance, T1 modality is more effective in observing gray matter in the brain, while FLAIR focuses on cerebrospinal fluid. These differences create semantic gaps between modalities, making alignment challenging. Despite these differences, multimodal data shares implicit associations as it represents the same underlying subject. To address this complexity, we propose a multimodal feature semantic alignment mechanism. This mechanism leverages a nonlinear transformation module to achieve deep interaction and semantic alignment between modalities, constructing a new unified feature representation space based on f_i.

We designed a nonlinear transformation module to achieve implicit interaction and semantic alignment between modalities:

$$f_i' = \mathcal{F}_{\text{Norm}}\left(\mathbf{W_1} \cdot f_i + \mathbf{b_1}\right), \tag{1}$$

$$f_i'' = \mathbf{W_2} \cdot \mathcal{F}_{\text{GELU}}(f_i') + \mathbf{b_2}, \tag{2}$$

where $\mathcal{F}_{\text{Norm}}$ denotes layer normalization, which is used for feature normalization to ensure semantic space alignment of features. $\mathcal{F}_{\text{GELU}}$ represents the activation function, capturing complex interactions between different modalities through nonlinear transformation. The second linear transformation remaps features to the original dimension, ensuring that the output features of each modality are influenced by all other modalities. This approach enables the model to interactively integrate features from all modalities adaptively. On the basis of integrating information from other modalities

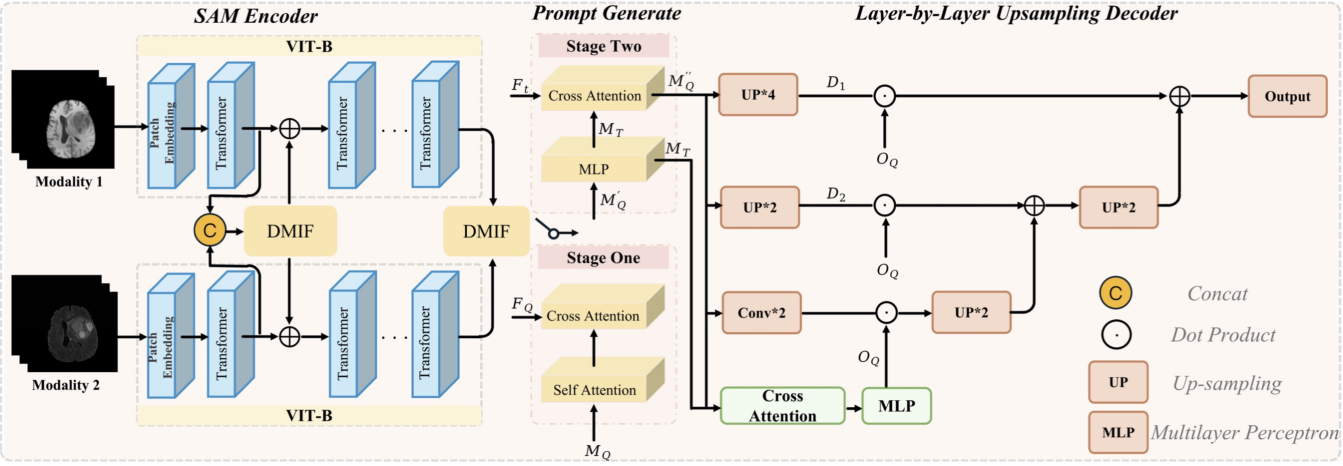

Figure 2: The schematic illustration of our BrainSegDMIF model designed for multimodal brain lesion segmentation. Given a sequence of multimodal brain lesion images, the DMIF module fuses multimodal features and encodes the multimodal images as input. A refined layer-by-layer upsampling decoder is employed to generate segmentation masks. Image features are fused with mask tokens through an attention mechanism, focusing on critical information within the masked features and capturing important characteristics of the lesion regions.

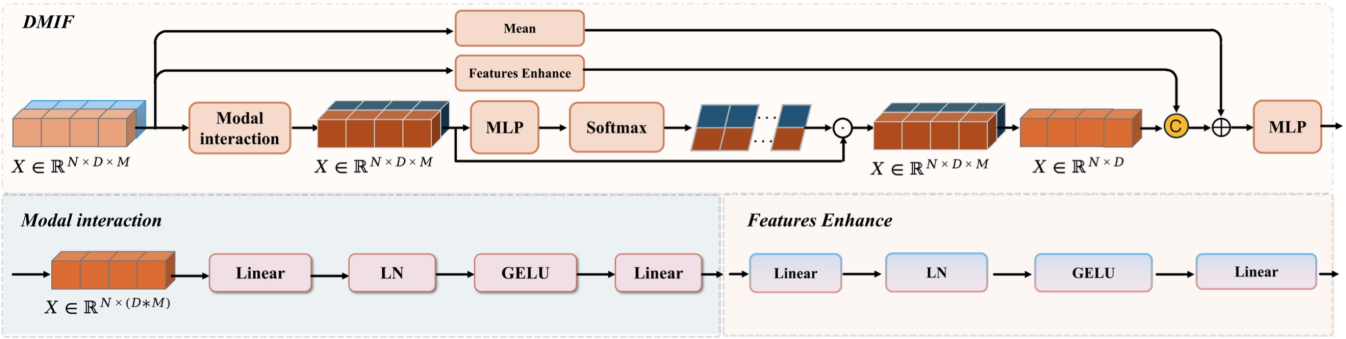

Figure 3: The figure presents the schematic of our Dynamic Modal Interactive Fusion (DMIF) module. This module accepts concatenated multi-modal image tokens. Through dynamic interactions, it fuses multi-modal information so that each token incorporates features from other modalities. Dynamic weights are generated to emphasize salient features and suppress redundancy. The fused features are then refined via these weights. Finally, the aggregated features are enhanced using a broadcasting mechanism with residual connections, yielding the final multi-modal features.

for each individual modality, the original feature information of each modality is retained.

3.1.2 Dynamic weight generation. In multimodal learning, significant differences in data visibility, noise levels, etc., can lead to neglect of statistical dependencies and information redundancy between modalities during feature fusion, causing representation quality degradation due to noise interference. To achieve precise modality feature fusion, we introduce an adaptive weight generation mechanism. By generating weights in each encoder component, it adaptively determines each modality's importance in each encoding state. These weights compile multimodal fusion representations in each encoding layer, as shown in Figure 3. First, the interactively fused multimodal features f_i'' are passed through a multi-layer fully connected network to learn feature weights at different encoding layers. Then, softmax normalization is applied to obtain each feature's percentage among all features. The resulting weights are multiplied with the corresponding feature vectors to obtain a multimodal feature $F_i \in \mathbb{R}^{N\times D}$ that adaptively adjusts feature distribution based on current needs. This feature, containing all features of the current encoding layer, effectively suppresses the impact of noise and irrelevant modalities on the model. The process is defined as:

$$\mathbf{W}_{model} = \sigma(MLP(f_i'')), \tag{3}$$

$$\sigma(x_i) = \frac{e^{x_i}}{\sum_{j=1}^{M} e^{x_j}} \quad for\ i = 1, 2, \ldots, M, \tag{4}$$

where $\mathbf{W}_{model}$ denotes the learned adaptive multimodal feature weight matrix, and $\sigma(\cdot)$ epresents the softmax function, ensuring

the generated weights sum to 1 to reflect each feature's importance. The generated weight matrix $\mathbf{W}_{model}$ is element-wise multiplied with the interactively fused features:

$$f_i''' = f_i'' \odot \mathbf{W}_{modal}, \tag{5}$$

where $\odot$ denotes the Hadamard product.

3.1.3 Feature Convergence. From the previous step, we obtained multimodal features f_i''' with varying feature distributions at each encoding step. These features can adaptively adjust themselves, but interaction between modalities has not yet been established, as interaction was only completed within the DMIF module. To transmit the interacted features to each modality encoding component, we summed the features obtained from the previous step to form the final fused multimodal feature $F_i \in \mathbb{R}^{N\times D}$:

$$F_i = \sum_{j=1}^{M} f_i'''[..., j], \tag{6}$$

this feature incorporates the importance of each modality at this layer. To maintain feature diversity, we designed parallel feature enhancement branches. These branches use a feature enhancement function $\gamma(\cdot)$ to extract useful information from the originally concatenated features through nonlinear transformations, constructing a representational subspace complementary to the main fusion path. This supplements the main aggregation path, and combining information from both paths yields complete multimodal information Fc . Finally, to ensure information integrity and gradient flow, we introduced a residual linear structure that uses the average representation of multimodal features:

$$f_{fus} = F_c + \frac{1}{M}\sum_{j=1}^{M} f_i[..., j], \tag{7}$$

this design ensures fairness of the residual branch in multimodal scenarios, preventing residual information from biasing toward specific modalities and enhancing the diversity of feature representation.

3.2 Prompt Generate

Since the SAM architecture relies on prompt-based mask generation, we designed a Prompt generate module to enable SAM to perform automatic lesion segmentation. By incorporating attention mechanisms, this module facilitates interaction between image tokens and mask tokens, allowing the generated mask tokens to capture key information related to lesions in the image. This approach enables the automatic learning of prompts associated with lesion regions, thereby achieving automatic segmentation.

The process is divided into two stages. In the first stage, we define the mask token as $M_Q \in \mathbb{R}^{N\times D}$, where N is the number of mask tokens and D is the feature dimension. We employ self-attention to learn the internal contextual information of the mask tokens. The attention-encoded mask tokens are represented as $\tilde{M}_Q$. Given the multimodal features $F_r \in \mathbb{R}^{N\times D}$, we compute the attention between $\tilde{M}_Q$ and F_r :

$$M_Q^{'} = \mathrm{Attn}(\tilde{M}_Q, F_r) = \mathrm{Softmax}\left(\frac{\tilde{M}_Q \tilde{W}_Q (F_r W_K^r)^T}{\sqrt{d_k}}\right) F_r W_V^r, \tag{8}$$

this establishes a relationship between the multimodal features and the mask tokens, aligning them semantically and enriching the mask tokens with missing information.

In the second stage, we pass $M_Q^{'}$ through a fully connected layer to obtain the final mask features $M_T \in \mathbb{R}^{N\times D}$ This enhances the model's expressiveness and aids in more complex processing. To enable the multimodal features to focus on key information in the mask features and capture lesion characteristics, we compute the attention between the multimodal features F_t and M_T :

$$M_Q'' = \mathrm{Attn}(F_t, M_T), \tag{9}$$

we thereby obtain the enhanced multimodal features $M_Q'' \in \mathbb{R}^{N\times D}$, which integrate mask information. These features serve as the input to the decoder, providing comprehensive multimodal information for the decoding process.

3.3 Layer-by-Layer Upsampling Decoder

Intracranial lesions often contain small pathological regions. Following data slicing, a single slice may contain tiny lesions. These small lesions are typically characterized by fuzzy boundaries and strong heterogeneity. To address these challenges, we designed a layer-wise upsampling decoder, as depicted in Figure 2. Our decoder comprises multiple upsampling and convolution modules.

The enhanced features M_Q'' are passed through upsampling modules of different sizes, utilizing 2D transposed convolution operations to obtain information at different resolutions, namely D_1 , D_2 , and D_3:

$$D_i = \mathcal{F}_{up}^i(M_Q'') = \mathrm{ConvTranspose2D}(M_Q''; \theta_i), \quad i \in 1, 2, 3 \tag{10}$$

where F_{up}^i enotes the i-th upsampling module, composed of transposed convolutions with different strides and kernel sizes. θ_i represents the learnable parameters of the module.

We integrate mask information M_T and image information M_Q'' via attention to form a comprehensive feature representation $O_Q \in \mathbb{R}^{N\times D}$, which captures interactions between mask and multimodal information. We then use O_Q to enhance the previously obtained multi-scale features D_1 , D_2 , and D_3 through feature modulation:

$$D_i^{enhanced} = G(O_Q) \odot D_i, \quad i \in 1, 2, 3 \tag{11}$$

where G is a feature mapping function that converts O_Q into a representation compatible with D_i , and $\odot$ denotes element-wise multiplication. This operation enables the model to adaptively emphasize key information in multi-scale features based on O_Q .

Finally, we resize $D_1^{enhanced}$ and $D_2^{enhanced}$ to the same spatial dimensions using bilinear interpolation and combine them with $D_3^{enhanced}$ to generate the final mask:

$$D_i^{resized} = I(D_i^{enhanced}, s_i), \quad i \in 1, 2 \tag{12}$$

where $I(\cdot, s_i)$ represents the bilinear interpolation function, and s_i is the scaling factor.

We fuse features across scales progressively:

$$D_{final} = D_1^{resized} + D_2^{resized} + D_3^{enhanced}, \tag{13}$$

this multi-scale feature fusion strategy enables our model to leverage spatial information at different resolutions, producing segmentation masks with clear boundaries and complete structures.

3.3.1 Loss function. To improve the model's performance in detecting small lesions, we adopted FocalDice Loss as the loss function. This loss function combines Focal Loss and Dice Loss, with a linear weighting ratio of 1:2, thereby enhancing sensitivity to small lesions. The calculation formula is as follows:

$$FocalDice = \frac{1}{2}Focal + Dice. \tag{14}$$

4 Experiments

4.1 Datasets and Evaluation Metrics

4.1.1 datasets. To evaluate the efficacy of our methodology, we employed three publicly available multi-sequence MRI datasets for segmentation tasks and ablation experiments. These datasets encompass various pathologies and multiple modalities including (disease types) and (modality names). The datasets are as follows:

BraTS21 (Brain Tumor Segmentation Challenge)[1]. This dataset represents a comprehensive, publicly available multi-modal brain glioma segmentation dataset, encompassing four MRI modalities: T1, T1Gd, T2, and T2-FLAIR. Each modality has dimensions of 240x240x155 (LxWxH). Ground truth annotations, created and approved by expert neuroradiologists, are provided for each subject. The dataset includes 8,160 MRI scans from 2,040 patients. Annotations comprise normal tissue regions and three tumor sub-regions: Enhancing Tumor (ET), Peritumoral Edema/Invaded Tissue (ED), and Necrotic Tumor Core (NCR). All labels and data have undergone preprocessing, including alignment with a standardized anatomical template, adjustment to uniform resolution (1 mm^3), and skull-stripping. The dataset allocates 1,251 cases for training, 219 for validation, and 570 for testing.

FCD2023[27]. This public dataset focuses on Focal Cortical Dysplasia (FCD) and includes three modalities: T1, T2, and FLAIR, from 85 patients. Data acquisition utilized a 32-channel head coil, with image dimensions of 256x256 and voxel size of 1.0 mm×1.0 mm×1.0 mm. All personally identifiable information has been removed from the dataset, and all data have been converted to NIfTI format.

Regarding image preprocessing, our model is designed for 2D image segmentation. We initially performed resampling and alignment of the multi-modal datasets, followed by slicing the 3D data along the third dimension and saving the resulting 2D slices. The provided mask data were adjusted to values within the [0-255] range.

4.1.2 Evaluation Metrics. Given that our model focuses on lesion segmentation, to objectively evaluate our model's performance, we selected four of the most commonly used metrics, Dice and IoU (Intersection over Union), as well as Precision and Recall, to fairly evaluate the performance of our model by comparing the final segmentation results. Dice measures the similarity between predicted results and ground-truth labels, while IoU represents the ratio of the intersection to the union of predicted results and ground-truth labels. Precision reflects the accuracy of the model in identifying true positives among all predicted positives, and Recall reflects the model's sensitivity to detecting true positives.

4.2 Implementation Details

Our method was implemented using the PyTorch deep learning framework and trained for 200 epochs on four NVIDIA A100 GPUs with 80GB of memory each. We employed the Adam optimizer with an initial learning rate of 1×10^{-4} and utilized a MultiStepLR learning rate scheduler to dynamically adjust the optimizer's learning rate. Specifically, the learning rate was multiplied by 0.5 at the 7th and 12th epochs to gradually reduce it, aiding model convergence. Due to memory constraints, we fine-tuned only the base model of SAM (SAM-B) in this work. During training, all images were resized to 256x256 resolution. If an image's width or height was smaller than 256, its borders were padded with black; otherwise, bilinear interpolation was used for resizing.

4.3 Comparisons With Other Methods

In this section, we conducted a quantitative comparison with several state-of-the-art methods, including UNETR[7], SwinUNETR[6], nnFormer[36], MixUNETR[28], STUNet[9], SAM 2[25], MedSAM[20], and SAMMed2D[4]. To ensure a fair comparison, the comparison models used the FLAIR modality data, which showed the best segmentation results in Table 1, and were trained according to their default training protocols. The quantitative comparison results are presented in Table , where our method demonstrates superior performance across all datasets. Specifically, on the BraTS2021 dataset, our method achieved a Dice score of 79.64, an IoU of 68.55, a Precision of 81.88, and a Sensitivity of 78.24, outperforming the second-best method, SAM Med2D, by 7.25, 5.34, 11.09, and 2.56 points, respectively. On the FCD 2023 dataset, our model achieved a Dice score of 64.84, an IoU of 51.07, a Precision of 63.79, and a Sensitivity of 68.07, surpassing SAM Med2D by 7.36, 8.11, 7.48, and 9.16 points, respectively. Compared to MedSAM, which also leverages SAM, our method achieved a Dice score that was 7.96 higher, an IoU that was 6.59 higher, a Precision that was 7.53 higher, and a Sensitivity that was 10.36 higher on the BraTS2021 dataset. The superior segmentation performance of our method can be attributed to modal interaction during training, enabling the model to learn domain knowledge from multimodal data and capture data from different perspectives. Figure 4 shows the segmentation results of various methods on the BraTS21 dataset, illustrating that our method better identifies lesion regions. Figure 5 presents the segmentation results of each method on the FCD2023 dataset, where our method more effectively distinguishes between lesion and non-lesion regions.

4.4 Ablation experiment

4.4.1 The Impact of Multimodal Data on Segmentation. We conducted ablation studies on each modality's impact on the model, as shown in Table 2. From the table, it is evident that using all modalities for segmentation yields the highest Dice, IoU, and Prec scores. When using three modalities, the combination of T2, T1CE, and FLAIR performs the best. However, adding a fourth modality (FALIR) leads to a lower Sens score compared to using three modalities. This confirms our assertion that not all information in each modality is beneficial for model learning.

4.4.2 The Effectiveness of DMIF, PG, and LUD. We conducted paired experiments to analyze the impact of our proposed modules on

Table 1: Quantitative results of different methods on BraTs2021 and FCD2023 in terms of Dice(%), IoU(%), Prec(%), Sens(%).Where Prec denotes Precision, and Sens denotes Recall. * indicates the use of a pre-trained model. MedSAM* and SAM Med2D* utilize their respective ViT-B pre-trained models.

#	Method	Year	Params / GF	BraTS2021				FCD2023				Average	
				Dice	IoU	Prec	Sens	Dice	IoU	Prec	Sens	Dice	IoU
1	UNETR	2022	112M / 270	52.26	48.09	56.75	49.32	26.68	16.09	33.45	25.56	39.47	32.09
2	SwinUNETR	2021	62M / 214	53.27	47.14	54.43	53.33	28.64	16.09	29.71	27.86	40.96	31.62
3	nnFormer	2021	149M / 119	62.36	54.80	63.50	61.45	43.88	30.35	46.91	45.61	53.12	42.58
4	MixUNETR	2025	50M / 228	61.98	52.14	59.65	62.31	38.61	24.52	35.56	41.72	50.30	38.33
5	STUNet	2023	8M / 24	59.80	51.06	60.32	57.11	27.42	16.75	28.81	26.18	43.61	33.91
6	SAM 2	2024	44M / 128	00.03	00.01	00.02	00.02	00.03	00.01	00.01	00.02	00.03	00.01
7	MedSAM*	2024	70M / 743	68.44	55.08	69.60	68.21	54.02	39.66	53.20	55.60	61.23	47.37
8	MedSAM	2024	70M / 743	71.68	61.96	74.35	67.88	56.43	40.77	51.20	58.61	64.06	51.37
9	SAM Med2D*	2024	271M / 130	70.89	58.95	72.51	66.28	55.83	45.25	57.31	53.17	63.36	52.10
10	SAM Med2D	2024	271M / 130	72.39	63.21	70.79	75.68	57.51	42.96	56.31	58.91	64.95	53.09
11	BrainSegDMIF	2025	354M / 311	**79.64**	**68.55**	**81.88**	**78.24**	**64.87**	**51.07**	**63.79**	**68.07**	**72.26**	**59.81**

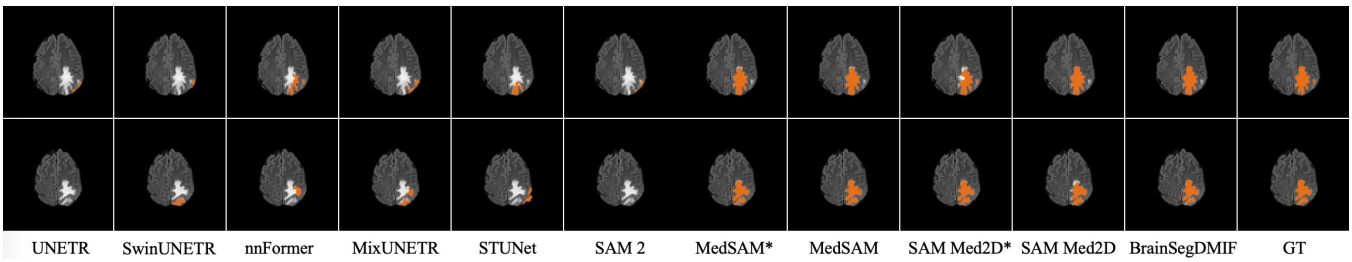

Figure 4: The visualization of our model's segmentation performance on the BraTs21 dataset is presented. * indicates the use of a pre-trained model.

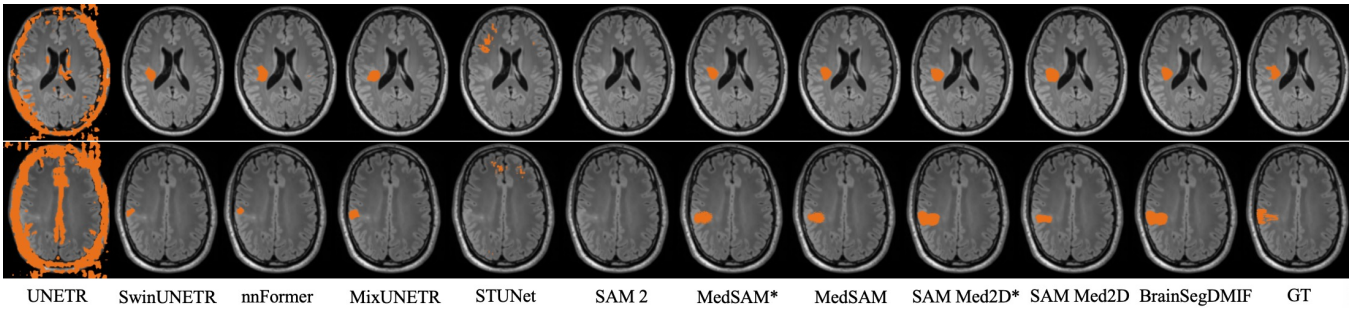

Figure 5: The visualization of segmentation results for various models on the FCD2023 dataset is presented. * indicates the use of a pre-trained model.

segmentation results. The model with only the PG module served as the baseline. From Table 3, it can be observed that the model without the DMIF module performed the worst across all four metrics. When only the PG module was used, the model achieved the lowest performance. After adding the LUD module, the Dice score improved by 3.07, the IoU metric increased by 6.02, the Prec metric rose by 0.76, and the Sens metric improved by 7.47. When the DMIF module was added, the model achieved the best performance. This demonstrates that the modules proposed in this study effectively enhance the segmentation performance of the model.

5 Conclusion

Our work proposes a novel network named BrainSegDMIF, based on SAM, which explores brain parenchymal lesion segmentation through multimodal fusion and layer-wise upsampling decoding. BrainSegDMIF introduces three key contributions: the multimodal fusion module (DMIF), a layer-wise upsampling decoder, and automatic image segmentation. The multimodal fusion module is integrated into the SAM Encoder, enabling it to learn features from multiple modalities during image encoding by interacting with multimodal data.

Table 2: The Impact of Multimodal Data on Segmentation

Modalities Input				*Metric*			
T1	T2	T1CE	FLAIR	*DICE*	*IoU*	*Prec*	*Sens*
✓	✓			73.84	64.27	70.29	76.53
✓		✓		72.33	62.89	74.61	71.10
✓			✓	72.58	63.56	73.12	72.19
	✓	✓		73.91	64.33	74.97	72.13
	✓		✓	74.16	61.36	75.34	73.79
✓	✓	✓		75.12	67.01	71.35	**78.97**
✓	✓		✓	74.56	65.78	80.43	70.38
✓		✓	✓	74.86	65.92	73.34	75.82
	✓	✓	✓	76.89	67.64	75.35	77.44
✓	✓	✓	✓	**79.64**	**68.55**	**81.78**	78.24

Table 3: The Effectiveness of DMIF, PG, and LUD, where DMIF stands for Dynamic Modal Interactive Fusion, PG refers to Prompt Generate, and LUD represents Layer-by-Layer Upsampling Decoder.

DMIF	PG	LUD	*DICE*	*IoU*	*Prec*	*Sens*
✓			74.53	63.71	76.29	70.26
	✓		71.29	58.45	72.77	67.94
		✓	73.93	60.28	71.08	75.34
✓	✓		75.80	65.91	79.05	73.67
✓		✓	76.75	65.88	80.51	75.29
	✓	✓	74.36	64.47	73.53	75.41
✓	✓	✓	**79.64**	**68.55**	**81.78**	**78.24**

Given the potential presence of small lesions in brain parenchymal diseases and the possibility of lesions appearing extremely small in image slices, we designed a layer-wise upsampling decoder. This decoder progressively enlarges feature scales and fuses multi-scale features, enhancing the model's sensitivity to small lesions and improving lesion segmentation accuracy. Additionally, by designing a prompt generator, we achieved fully automatic lesion segmentation.

Experimental results on the BraTS21 and FCD 2023 datasets demonstrate that our network effectively integrates multimodal data, comprehensively learns data features, and achieves superior segmentation accuracy.

References

[1] Ujjwal Baid, Satyam Ghodasara, Suyash Mohan, Michel Bilello, Evan Calabrese, Errol Colak, Keyvan Farahani, Jayashree Kalpathy-Cramer, Felipe C Kitamura, Sarthak Pati, et al. 2021. The rsna-asnr-miccai brats 2021 benchmark on brain tumor segmentation and radiogenomic classification. *arXiv preprint arXiv:2107.02314* (2021).

[2] Olivier Bernard, Alain Lalande, Clement Zotti, Frederick Cervenansky, Xin Yang, Pheng-Ann Heng, Irem Cetin, Karim Lekadir, Oscar Camara, Miguel Angel Gonzalez Ballester, et al. 2018. Deep learning techniques for automatic MRI cardiac multi-structures segmentation and diagnosis: is the problem solved? *IEEE transactions on medical imaging* 37, 11 (2018), 2514–2525.

[3] Hu Cao, Yueyue Wang, Joy Chen, Dongsheng Jiang, Xiaopeng Zhang, Qi Tian, and Manning Wang. 2022. Swin-unet: Unet-like pure transformer for medical image segmentation. In *European conference on computer vision*. Springer, 205–218.

[4] Junlong Cheng, Jin Ye, Zhongying Deng, Jianpin Chen, Tianbin Li, Haoyu Wang, Yanzhou Su, Ziyan Huang, Jilong Chen, Lei Jiang, et al. 2023. Sam-med2d. *arXiv preprint arXiv:2308.16184* (2023).

[5] Guoyao Deng, Ke Zou, Kai Ren, Meng Wang, Xuedong Yuan, Sancong Ying, and Huazhu Fu. 2023. Sam-u: Multi-box prompts triggered uncertainty estimation for reliable sam in medical image. In *International Conference on Medical Image Computing and Computer-Assisted Intervention*. Springer, 368–377.

[6] Ali Hatamizadeh, Vishwesh Nath, Yucheng Tang, Dong Yang, Holger R Roth, and Daguang Xu. 2021. Swin unetr: Swin transformers for semantic segmentation of brain tumors in mri images. In *International MICCAI brainlesion workshop*. Springer, 272–284.

[7] Ali Hatamizadeh, Yucheng Tang, Vishwesh Nath, Dong Yang, Andriy Myronenko, Bennett Landman, Holger R Roth, and Daguang Xu. 2022. Unetr: Transformers for 3d medical image segmentation. In *Proceedings of the IEEE/CVF winter conference on applications of computer vision*. 574–584.

[8] Ali Hatamizadeh, Hongxu Yin, Greg Heinrich, Jan Kautz, and Pavlo Molchanov. 2023. Global context vision transformers. In *International Conference on Machine Learning*. PMLR, 12633–12646.

[9] Ziyan Huang, Haoyu Wang, Zhongying Deng, Jin Ye, Yanzhou Su, Hui Sun, Junjun He, Yun Gu, Lixu Gu, Shaoting Zhang, et al. 2023. Stu-net: Scalable and transferable medical image segmentation models empowered by large-scale supervised pre-training. *arXiv preprint arXiv:2304.06716* (2023).

[10] Fabian Isensee, Paul F Jaeger, Simon AA Kohl, Jens Petersen, and Klaus H Maier-Hein. 2021. nnU-Net: a self-configuring method for deep learning-based biomedical image segmentation. *Nature methods* 18, 2 (2021), 203–211.

[11] Fabian Isensee, Paul F Jäger, Simon AA Kohl, Jens Petersen, and Klaus H Maier-Hein. 2019. Automated design of deep learning methods for biomedical image segmentation. *arXiv preprint arXiv:1904.08128* (2019).

[12] Zeyu Jiang, Changxing Ding, Minfeng Liu, and Dacheng Tao. 2020. Two-stage cascaded u-net: 1st place solution to brats challenge 2019 segmentation task. In *Brainlesion: Glioma, Multiple Sclerosis, Stroke and Traumatic Brain Injuries: 5th International Workshop, BrainLes 2019, Held in Conjunction with MICCAI 2019, Shenzhen, China, October 17, 2019, Revised Selected Papers, Part I 5*. Springer, 231–241.

[13] Leo Joskowicz, D Cohen, N Caplan, and Jacob Sosna. 2019. Inter-observer variability of manual contour delineation of structures in CT. *European radiology* 29 (2019), 1391–1399.

[14] Alain Jungo, Raphael Meier, Ekin Ermis, Marcela Blatti-Moreno, Evelyn Herrmann, Roland Wiest, and Mauricio Reyes. 2018. On the effect of inter-observer variability for a reliable estimation of uncertainty of medical image segmentation. In *Medical Image Computing and Computer Assisted Intervention–MICCAI 2018: 21st International Conference, Granada, Spain, September 16-20, 2018, Proceedings, Part I*. Springer, 682–690.

[15] Alexander Kirillov, Eric Mintun, Nikhila Ravi, Hanzi Mao, Chloe Rolland, Laura Gustafson, Tete Xiao, Spencer Whitehead, Alexander C Berg, Wan-Yen Lo, et al. 2023. Segment anything. In *Proceedings of the IEEE/CVF international conference on computer vision*. 4015–4026.

[16] Tim J Kruser, Walter R Bosch, Shahed N Badiyan, Joseph A Bovi, Amol J Ghia, Michelle M Kim, Abhishek A Solanki, Sean Sachdev, Christina Tsien, Tony JC Wang, et al. 2019. NRG brain tumor specialists consensus guidelines for glioblastoma contouring. *Journal of neuro-oncology* 143 (2019), 157–166.

[17] Yu Liu, Fuhao Mu, Yu Shi, and Xun Chen. 2022. Sf-net: A multi-task model for brain tumor segmentation in multimodal mri via image fusion. *IEEE Signal Processing Letters* 29 (2022), 1799–1803.

[18] Zhihua Liu, Lei Tong, Long Chen, Zheheng Jiang, Feixiang Zhou, Qianni Zhang, Xiangrong Zhang, Yaochu Jin, and Huiyu Zhou. 2023. Deep learning based brain tumor segmentation: a survey. *Complex & intelligent systems* 9, 1 (2023), 1001–1026.

[19] Wenjie Luo, Yujia Li, Raquel Urtasun, and Richard Zemel. 2016. Understanding the effective receptive field in deep convolutional neural networks. *Advances in neural information processing systems* 29 (2016).

[20] Jun Ma, Yuting He, Feifei Li, Lin Han, Chenyu You, and Bo Wang. 2024. Segment anything in medical images. *Nature Communications* 15, 1 (2024), 654.

[21] Andriy Myronenko. 2018. 3D MRI brain tumor segmentation using autoencoder regularization. In *International MICCAI brainlesion workshop*. Springer, 311–320.

[22] Maximilian Niyazi, Michael Brada, Anthony J Chalmers, Stephanie E Combs, Sara C Erridge, Alba Fiorentino, Anca L Grosu, Frank J Lagerwaard, Giuseppe Minniti, René-Olivier Mirimanoff, et al. 2016. ESTRO-ACROP guideline "target delineation of glioblastomas". *Radiotherapy and oncology* 118, 1 (2016), 35–42.

[23] Maithra Raghu, Thomas Unterthiner, Simon Kornblith, Chiyuan Zhang, and Alexey Dosovitskiy. 2021. Do vision transformers see like convolutional neural networks? *Advances in neural information processing systems* 34 (2021), 12116–12128.

[24] Maithra Raghu, Chiyuan Zhang, Jon Kleinberg, and Samy Bengio. 2019. Transfusion: Understanding transfer learning for medical imaging. *Advances in neural information processing systems* 32 (2019).

[25] Nikhila Ravi, Valentin Gabeur, Yuan-Ting Hu, Ronghang Hu, Chaitanya Ryali, Tengyu Ma, Haitham Khedr, Roman Rädle, Chloe Rolland, Laura Gustafson, et al. 2024. Sam 2: Segment anything in images and videos. *arXiv preprint arXiv:2408.00714* (2024).

[26] Olaf Ronneberger, Philipp Fischer, and Thomas Brox. 2015. U-net: Convolutional networks for biomedical image segmentation. In *Medical image computing and computer-assisted intervention–MICCAI 2015: 18th international conference, Munich, Germany, October 5-9, 2015, proceedings, part III 18*. Springer, 234–241.

[27] Fabiane Schuch, Lennart Walger, Matthias Schmitz, Bastian David, Tobias Bauer, Antonia Harms, Laura Fischbach, Freya Schulte, Martin Schidlowski, Johannes Reiter, et al. 2023. An open presurgery MRI dataset of people with epilepsy and focal cortical dysplasia type II. *Scientific Data* 10, 1 (2023), 475.

[28] Quanyou Shen, Bowen Zheng, Wenhao Li, Xiaoran Shi, Kun Luo, Yuqian Yao, Xinyan Li, Shidong Lv, Jie Tao, and Qiang Wei. 2025. MixUNETR: A U-shaped network based on W-MSA and depth-wise convolution with channel and spatial interactions for zonal prostate segmentation in MRI. *Neural Networks* 181 (2025), 106782.

[29] Guotai Wang, Wenqi Li, Sébastien Ourselin, and Tom Vercauteren. 2018. Automatic brain tumor segmentation using cascaded anisotropic convolutional neural networks. In *Brainlesion: Glioma, Multiple Sclerosis, Stroke and Traumatic Brain Injuries: Third International Workshop, BrainLes 2017, Held in Conjunction with MICCAI 2017, Quebec City, QC, Canada, September 14, 2017, Revised Selected Papers 3*. Springer, 178–190.

[30] Junde Wu, Ziyue Wang, Mingxuan Hong, Wei Ji, Huazhu Fu, Yanwu Xu, Min Xu, and Yueming Jin. 2025. Medical sam adapter: Adapting segment anything model for medical image segmentation. *Medical image analysis* (2025), 103547.

[31] Yifeng Wu, Xiaodong Zhang, Haoran Zhang, Yang Sun, Lin Li, Fengjun Zhu, Dezhi Cao, and Jinping Xu. 2024. Mamba-SAM: An Adaption Framework for Accurate Medical Image Segmentation. In *2024 IEEE International Conference on Bioinformatics and Biomedicine (BIBM)*. IEEE, 3856–3859.

[32] Chaoning Zhang, Fachrina Dewi Puspitasari, Sheng Zheng, Chenghao Li, Yu Qiao, Taegoo Kang, Xinru Shan, Chenshuang Zhang, Caiyan Qin, Francois Rameau, et al. 2023. A survey on segment anything model (sam): Vision foundation model meets prompt engineering. *arXiv preprint arXiv:2306.06211* (2023).

[33] Kaidong Zhang and Dong Liu. 2023. Customized segment anything model for medical image segmentation. *arXiv preprint arXiv:2304.13785* (2023).

[34] Yichi Zhang, Zhenrong Shen, and Rushi Jiao. 2024. Segment anything model for medical image segmentation: Current applications and future directions. *Computers in Biology and Medicine* (2024), 108238.

[35] Yao Zhang, Jiawei Yang, Jiang Tian, Zhongchao Shi, Cheng Zhong, Yang Zhang, and Zhiqiang He. 2021. Modality-aware mutual learning for multi-modal medical image segmentation. In *Medical Image Computing and Computer Assisted Intervention–MICCAI 2021: 24th International Conference, Strasbourg, France, September 27–October 1, 2021, Proceedings, Part I 24*. Springer, 589–599.

[36] Hong-Yu Zhou, Jiansen Guo, Yinghao Zhang, Xiaoguang Han, Lequan Yu, Liansheng Wang, and Yizhou Yu. 2023. nnFormer: volumetric medical image segmentation via a 3D transformer. *IEEE transactions on image processing* 32 (2023), 4036–4045.